Crosslinker-Induced Effects on the Gelation Pathway of a Low Molecular Weight Hydrogel

Noteborn, Willem E.M.; Zwagerman, Damy N.H.; Talens, Victorio Saez; Maity, Chandan; van der Mee, Lars; Poolman, Jos M.; Mytnyk, Serhii; van Esch, Jan H.; Eelkema, Rienk; More Authors

DOI
10.1002/adma.201603769

Publication date
2017

Document Version
Final published version

Published in
Advanced Materials

COMMUNICATION

Crosslinker-Induced Effects on the Gelation Pathway of a Low Molecular Weight Hydrogel

*Willem E. M. Noteborn, Damy N. H. Zwagerman, Victorio Saez Talens, Chandan Maity, Lars van der Mee, Jos M. Poolman, Serhii Mytnyk, Jan H. van Esch, Alexander Kros, Rienk Eelkema, and Roxanne E. Kieltyka**

The field of supramolecular materials strives to prepare functional scaffolds for a range of applications from biomedicine to electronics.[1–4] Specific properties of these materials such as adaptiveness, responsiveness, and recyclability can be ascribed to the supramolecular nature of their interactions over several length scales starting from monomers until the final self-assembled material. However, a caveat of their supramolecular nature is that they are often mechanically weak.[5–9] Several groups have recently disclosed the use of polymeric crosslinkers in supramolecular hydrogel materials composed of fibrillar aggregates to increase their mechanical properties by decoration with matched self-assembling units to the parent assembly or postmodification through covalent or noncovalent crosslinking strategies.[7,10–15] Commonly, the addition of polymeric crosslinkers results in an improvement of the material's mechanical properties; however, competition between intra- and interfibrillar crosslinking can occur preventing them from reaching their full mechanical potential.[13] Nonetheless, it can also be envisaged that changes to the underlying supramolecular polymer network may occur when a crosslinker is added, greatly impacting the final material properties.

Supramolecular materials composed of low molecular weight gelators (LMWGs) are of interest for use as biomedical materials,[16–21] biosensors,[22,23] optoelectronics,[24–26] and personal care products,[27] due to their facile preparation and stimuli-responsive character. The rational design of these molecules remains still nontrivial due to a lack of understanding of how their self-assembly occurs over several length scales to provide a macroscopic material.[28,29] Numerous studies reveal the importance of nucleation and fiber branching events that occur during the self-assembly process on the final gel properties.[6,28,30,31] The primary rate of fiber nucleation determines the amount of nuclei formed and the degree of branching.[30] These processes can dictate both fiber segment length and individual fiber network compactness, in which more overlapping individual fiber networks result in their greater interpenetration to provide stiffer materials. Simple surfactants and polymers that interact with the growing fibers[32] or increase the solution viscosity[33] have been demonstrated to affect these processes variably, with the possibility to increase or decrease mechanical properties of the resultant gel material. Therefore, there is a need to examine the effect of complex functional supramolecular modules on the self-assembly pathways of multicomponent low molecular weight gelating systems to advance their use in numerous applications.

Supramolecular materials formed by reaction-coupled self-assembly[34–36] provide an additional handle to control primary nucleation and fiber branching phenomena of low molecular weight hydrogelators by relying on reaction rate of the components. Van Esch and Eelkema reported the reaction-coupled self-assembly of a supramolecular hydrogel material by reacting a cyclohexane trishydrazide (hydrazide, compound **3**) and three aldehyde-containing bis(diethylene glycol) benzaldehyde (aldehyde, compound **4**) wedges to form **7**, whose subsequent gelation pathway was affected by the nature of the catalyst used.[36] A comparison of the hydrazone-forming reaction between gelator components at pH 5 and 7 showed distinct changes in the mechanical properties of the network consistent with differences in the hydrogel microstructure, thus demonstrating the importance of reaction rate on this process. In order to exploit such reaction-coupled materials for biomedical applications, control over mechanical properties and ligand presentation becomes important. We became thus interested in studying the effect of various (bio)polymeric crosslinkers on the self-assembly process of this reaction-coupled hydrazide-aldehyde gelator into hydrogel materials as a model system (**Scheme 1**). We selected duplex DNA (**1**), which acts as a stiff, negatively charged rigid rod below its persistence length (P = 50 nm, 150 bp)[37] ideal for the construction of (nano)materials,[38–40] and compared it against a soft, neutral poly(ethylene glycol) (PEG) polymer (P = 0.37 nm,[41] 10 kDa) (**2**) of comparable size. Aldehyde moieties were specifically incorporated at the terminal ends of the (bio)polymers (**1** and **2**) to introduce them during the self-assembly of the reaction-coupled network composed of **3** and **4**. We examined the effect of these two crosslinkers on the gelation of the reaction-coupled monomers into hydrogels

W. E. M. Noteborn, D. N. H. Zwagerman, V. Saez Talens, Prof. A. Kros, Dr. R. E. Kieltyka
Department of Supramolecular and Biomaterials Chemistry
Leiden Institute of Chemistry
Leiden University
P.O. Box 9502, 2300 RA, Leiden, The Netherlands
E-mail: r.e.kieltyka@chem.leidenuniv.nl
Dr. C. Maity, L. van der Mee, J. M. Poolman, S. Mytnyk, Prof. J. H. van Esch, Dr. R. Eelkema
Advanced Soft Matter Group
Department of Chemical Engineering
Delft University of Technology
Van der Maasweg 9, 2629 HZ, Delft, The Netherlands

DOI: 10.1002/adma.201603769

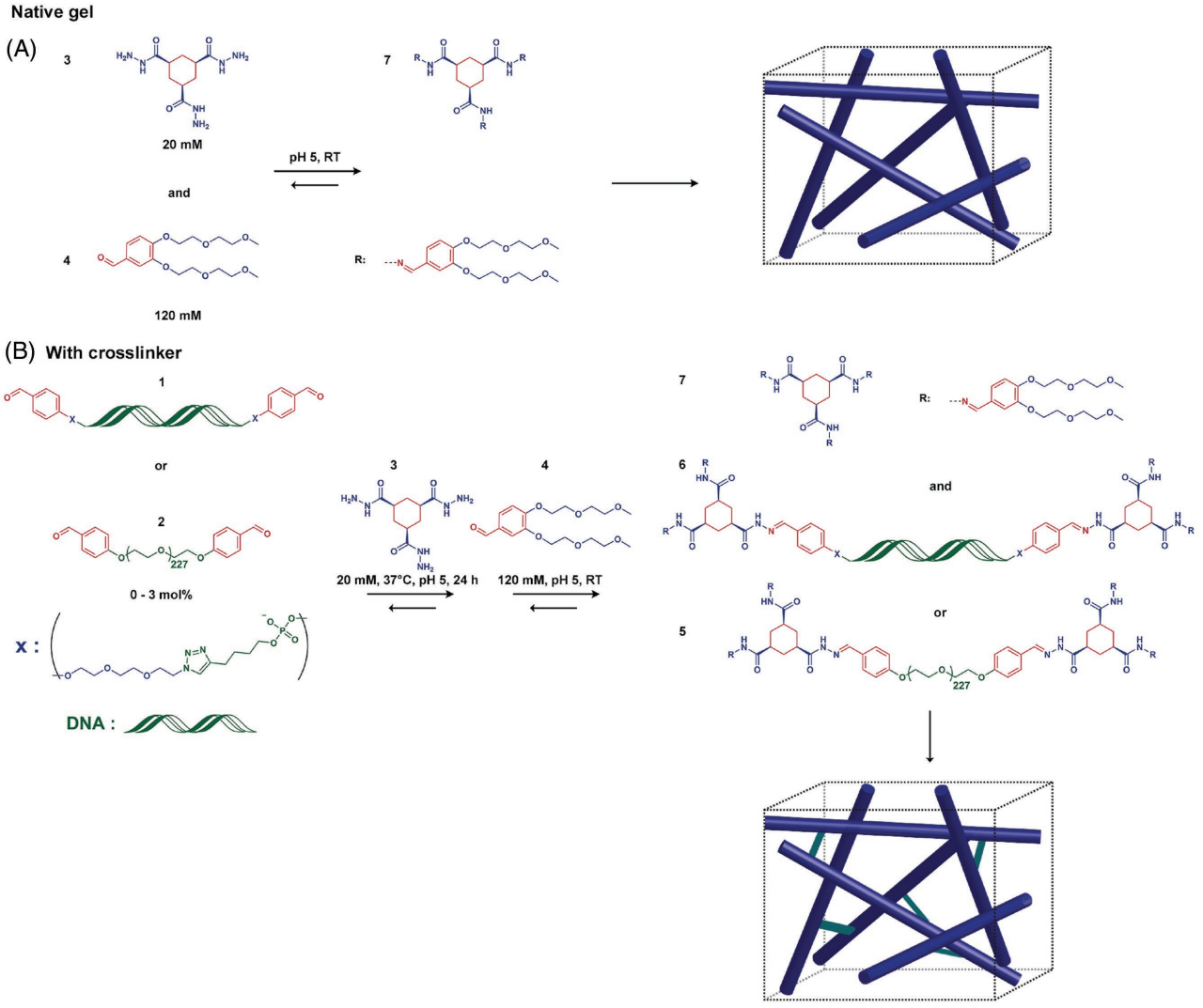

Scheme 1. Preparation of a reaction-coupled low molecular weight gelator network with (bio)polymeric crosslinkers under catalytic control. A) The native gel is synthesized by reacting hydrazide (**3**) and aldehyde (**4**) at pH 5 at room temperature. B) The biopolymeric crosslinked hydrogel is synthesized by reacting 5′-bisaldehyde functionalized dsDNA (20-mer) **1** or PEG **2** crosslinker (0–3 mol%), hydrazide **3** (20×10^{-3} M) over 24 h, and then aldehyde **4** (120×10^{-3} M) at pH 5 leading to native or crosslinked gel networks.

over several length scales and compared their resultant materials properties.

To chemically ligate either DNA (20-mer, length ≈ 6 nm) or PEG (M_n = 10 kDa, R_h ≈ 3 nm)[42] crosslinkers to the hydrazide-aldehyde network, we first introduced aldehyde moieties synthetically at their terminal ends by polymer-specific approaches. Moreover, circular dichroism and thermal denaturation studies of the crosslinker **1** showed similar characteristics to the unfunctionalized B-DNA duplex (for detailed synthesis and characterization see the Supporting Information). Originally, the hydrazide-aldehyde two-component hydrogel system was formed using a one-pot synthetic strategy by mixing hydrazide **3** and aldehyde **4** in a 1:6 molar ratio (20×10^{-3} M **3**: 120×10^{-3} M **4**) in 0.1 M phosphate buffer at pH 5 to yield a self-assembled network of **7** on the order of minutes.[43] Therefore, the concentration and ratio of aldehyde and hydrazide were conserved to maintain their rate of reaction[36] and the effect of reaction time of crosslinkers **1** or **2** with **3** on the formation and properties of the hydrogel network was probed in the present work. Using oscillatory rheology (see the Supporting Information), a self-assembly protocol was developed where crosslinkers **1** and **2** were required to be first reacted individually with **3** for 24 h at 37 °C and then mixed with **4** at room temperature. This protocol was further supported by a combination of matrix-assisted laser desorption/ionization time-of-flight mass spectrometry (MALDI-TOF-MS), gel electrophoresis (crosslinker **1**) and NMR (crosslinker **2**) studies over the various reaction steps (see the Supporting Information) to form the low molecular weight gelator material showcasing the potential for incorporation of the (bio)polymeric crosslinkers into the reaction-coupled network.

Once the reaction conditions were optimized for hydrazone formation of the various components (DNA **1** or PEG **2** crosslinkers combined with hydrazide **3**, and then aldehyde **4**) at

pH 5, the effect of reacting physicochemically distinct (bio)polymeric crosslinkers into the reaction-coupled supramolecular materials was explored. Oscillatory rheology was employed as a first approach to probe mechanical differences in the variably crosslinked materials, by examining time sweep profiles and comparing their final gel properties. Reaction of **3** (20×10^{-3} M) and **4** (120×10^{-3} M) in a 1:6 molar ratio without any added crosslinker provided a hydrogel material, which started to gelate with a steep increase after 7 min and showed a maximum storage modulus (G') (48 ± 8 kPa) after 50 min. Gelation using the 5′-bisaldehyde dsDNA crosslinker **1** resulted in variable changes in mechanical properties of the LMWG network, relative to the native network, depending on the amount of DNA added (**Figure 1**A). When 1 mol% of crosslinker **1** was added to the reaction-coupled assembly, a maximum in the mechanical properties was recorded with a striking 4.5-fold increase in storage modulus (209 ± 8 kPa). In this case, gelation started earlier, after 5 min, with an initial steep increase followed by a slower increase in the later stages and reaching a maximum in its storage modulus after 90 min. However, using a larger relative amount of DNA crosslinker **1** (3 mol%), the onset of gelation was strongly retarded, only starting after 20 min and showing a shallow increase in mechanical stiffness over the measuring range. A plateau was not detected, however the maximum storage modulus (36 ± 6 kPa) attained after 100 min was slightly below the native hydrazide-aldehyde hydrogel (48 ± 8 kPa).

As a control, a 5′-aldehyde functionalized ssDNA was hybridized with its complementary sequence bearing no reactive group at its 5′-end to compare its effect on the reaction-coupled self-assembly of the hydrazide-aldehyde gelator system relative to crosslinker **1**. The asymmetrically functionalized dsDNA when added at 1 mol% to **3** and then reacted with **4** to form the hydrazide-aldehyde hydrogel resulted in materials of lower mechanical stiffness (120 ± 20 kPa). When 5′-aldehyde ssDNA was reacted with **3**, and then **4**, materials of even lower mechanical stiffness (ssDNA: 60 ± 12 kPa) were synthesized relative to those with crosslinker **1**, but the storage modulus was still greater than the native gel (Figure S7, Supporting Information). To better understand the effect of DNA on the network, an endonuclease operative at pH 5, DNaseII, was added to the 5′-bisaldehyde dsDNA crosslinker **1** with **3** for 24 h prior to the addition of **4** to form the hydrogel network. The storage modulus of the obtained hydrogel with 1 mol% of **1** was reduced by half, indicative of enzymatic degradation of the DNA crosslinks (Figure 1C). However, the storage modulus after enzyme addition was still greater than that of a native gel.

Much to our surprise, based on earlier reports of PEG-based crosslinkers[11,13,15] enhancing properties of supramolecular hydrogels, crosslinker **2** showed a decrease in mechanical properties over the entire concentration range as examined for DNA with an even greater negative impact on the modulus of the material when increasing its concentration. For example, addition of 1 mol% **2** directly resulted in weaker materials in comparison to the native gel with a storage modulus of 29 ± 9 kPa (Figure 1B), despite a slightly earlier onset of gelation at 6 min with a sigmoidal profile. Overall, these results indicate that the physicochemical characteristics of the crosslinker and its concentration can have important consequences on the rate of low molecular weight hydrogel formation and its final mechanical properties. However, based on evidence from control samples and enzymatic degradation, the incorporation of the various

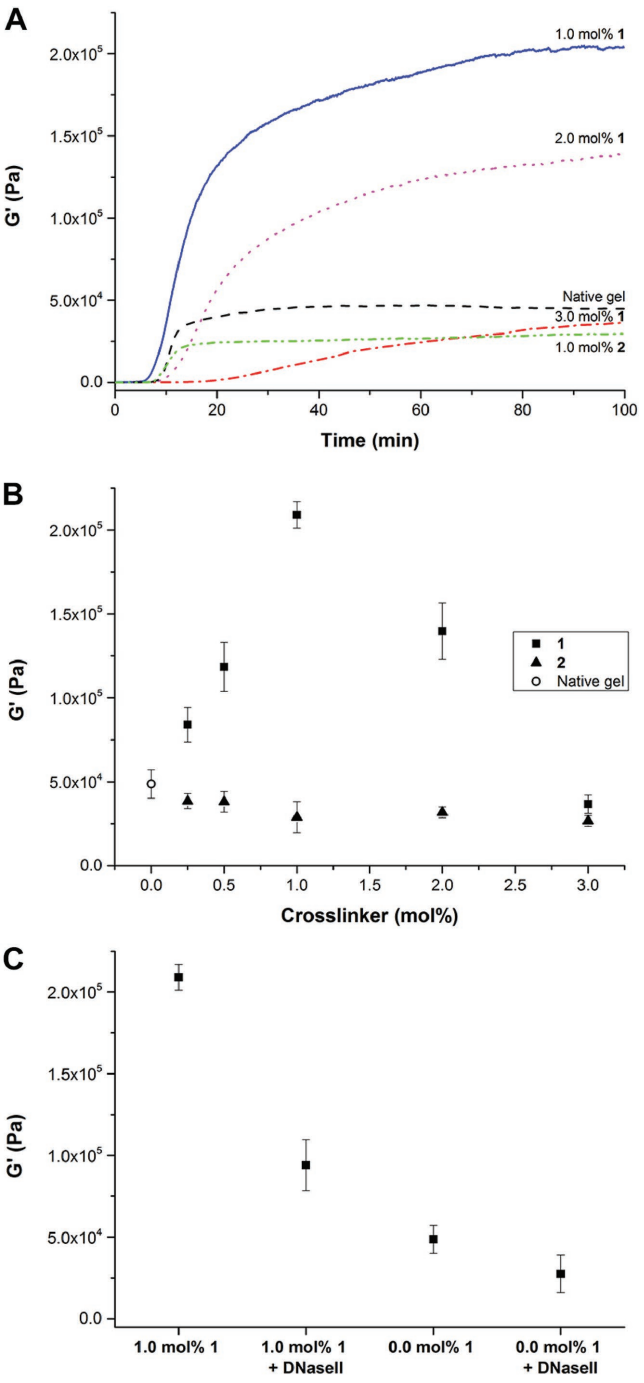

Figure 1. Oscillatory rheology data of reaction-coupled self-assembled hydrogels with various crosslinkers at pH 5. A) Time sweep measurements with **1** (native gel: black dashed, 1 mol%: blue continuous, 2 mol%: pink dotted, 3 mol%: red dashed-dotted) and **2** (1 mol%: green dashed-dotted) at 0.05% strain, 1 Hz frequency. B) Comparison of maximum measured storage moduli (G') of hydrogels containing DNA **1** (squares) and PEG **2** (triangles)-based crosslinkers as a function of concentration. C) Comparison of mechanical stiffness after degradation of 5′-bisaldehyde dsDNA crosslinks with DNaseII prior to the start of reaction-coupled self-assembly with **3**.

crosslinkers into the network does not entirely account for the changes observed in the mechanical properties. Therefore, insight into the effect of the crosslinkers on the reaction-coupled self-assembly process is necessary.

Low molecular weight hydrogel formation is majorly governed by the kinetic rate of fiber formation and percolation, which is dictated by nucleation, branching, and growth.[30] The dimensionality of fiber growth and branching in the presence of various crosslinkers using the Avrami equation before the onset of network percolation can be measured using the complex modulus, G^*, in the early stages of the rheological profile with respect to time (see Figure S8, Supporting Information). The dimensionality of growth can then be assessed by solving for the Avrami coefficient.[44] Fitting the Avrami equation for the native hydrogel system lacking any crosslinker resulted in $n = 1.31$, suggestive of branched fibrillar growth. Addition of 1.0 mol% stiff DNA crosslinker **1** yields $n = 1.70$, indicating a higher degree of fiber branching. Conversely, the use of 3.0 mol% **1** results in a value of $n = 0.76$, which suggests 1D or even growth that is hindered by the elimination of branching events. Analysis of the addition of 1.0 mol% **2** provides an $n = 1.02$, also suggestive of 1D unbranched growth. Collectively, the Avrami coefficients suggest a strong influence of the crosslinker identity on the nucleation and fiber formation processes.

Scanning electron (SEM, **Figure 2**), confocal laser scanning (CLSM), and cryogenic-transmission electron (cryo-TEM, Figure S11, Supporting Information) microscopies were used to gain insight into the hydrogel micro- and nanostructure with the various crosslinker concentrations to better understand the origin of the observed mechanical properties of the crosslinked materials. In the case of the native (compound **3** and **4** only) and 1.0 mol% DNA gels, dense, thin, highly branched fiber networks were observed by SEM (Figure 2A,B) and CLSM in the hydrated state, albeit at a lower magnification (Figure 2E,F). CLSM samples were stained with Nile Red (6.25×10^{-6} M), a lipophilic dye to visualize the hydrophobic interior of the aggregates. Conversely, less dense, thicker fibrils alongside spherical aggregates were found upon increasing the DNA content to 3 mol% (Figure 2C,G), whereas the addition of 1.0 mol% PEG-based crosslinker **2** resulted in a lack of well-defined fibrillar features with a larger surface in comparison to the native and 1.0 mol% DNA gel (Figure 2D,H). These images suggest that low concentrations of **1** (≈1 mol%) support growth of long interpenetrating fiber networks, while higher concentrations of **1** or the addition of **2** trigger the formation of smaller, spherical or collapsed networks respectively, with either scenario abolishing the rheological properties of the material. Subsequently, cryo-TEM images were made of the various crosslinked gels to examine the effect of the added polymer on the fibrillar architecture after self-assembly (Figure S11, Supporting Information). Near micrometer-long fibers were imaged in all samples. These results suggest that formation of fibers at the nanoscale remains unaffected regardless of the crosslinker used but highlights the importance of the assembly processes that occur at larger length scales. Therefore, both SEM and CLSM images of the supramolecular hydrogel microstructure with the various crosslinkers support the mechanical data obtained by oscillatory rheology.

Intrigued by the influence of the various crosslinkers on the hydrogel microstructure, their unique gelation profiles and mechanical properties measured by oscillatory rheology, we sought to investigate the process of network formation in real-time by CLSM (**Figure 3**). In the case of the native gel, addition

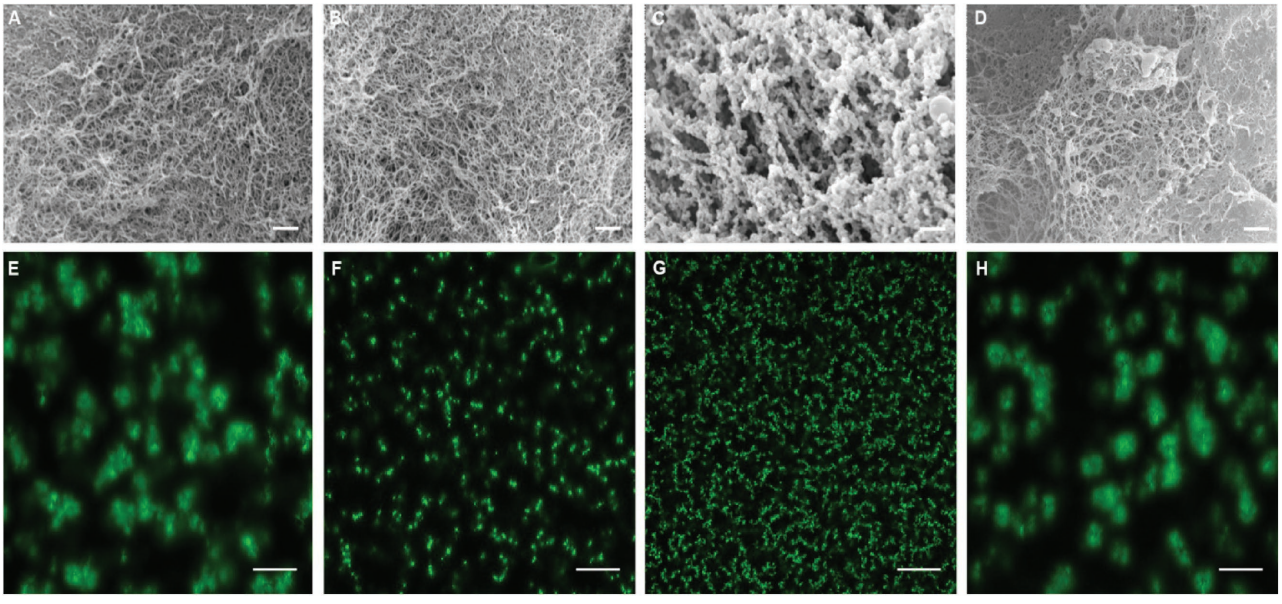

Figure 2. Visualization of the effect crosslinkers **1** and **2** on the reaction-coupled self-assembled aldehyde-hydrazide hydrogel microstructure by scanning electron (SEM) and confocal laser scanning (CLSM) microscopies. Scanning electron images of hydrogels A) without crosslinker, B) 1 mol% **1**, C) 3 mol% **1**, and D) 1 mol% **2**. All SEM samples were prepared by critical point drying. Scale bar is 1 µm. Confocal laser scanning images of hydrogels E) without crosslinker, F) 1 mol% **1**, G) 3 mol% **1**, and H) 1 mol% **2**. All CLSM samples were prepared in the presence of Nile Red (6.25×10^{-6} M) as a fluorescent probe. $\lambda_{ex} = 488$ nm, scale bar is 50 µm.

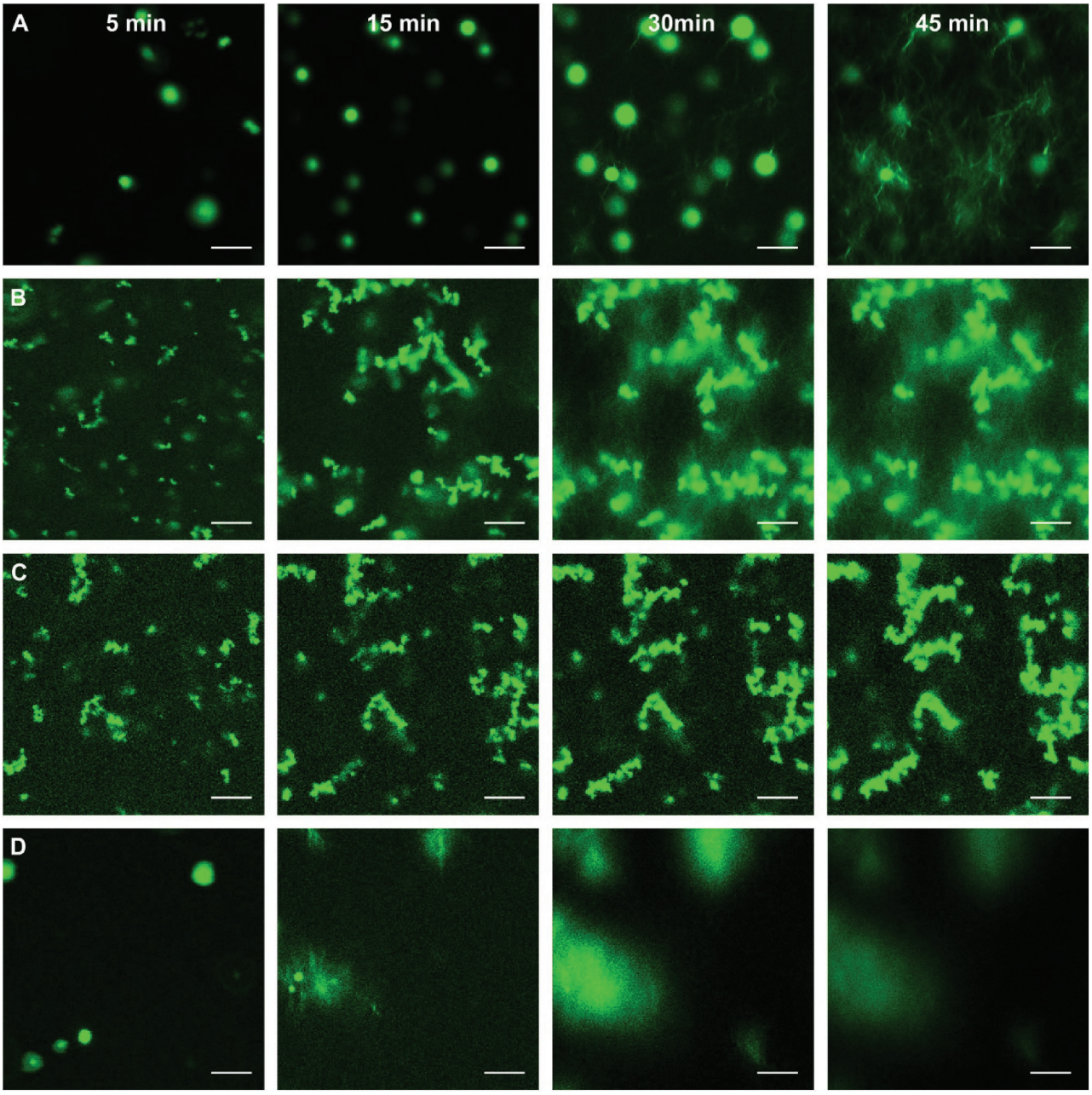

Figure 3. Time-lapsed confocal laser scanning microscopy (CLSM) images of the effect of crosslinkers **1** and **2** on the reaction-coupled self-assembly of the aldehyde-hydrazide hydrogel. Images of the various hydrogels were taken at different time intervals (5, 15, 30, and 45 min) after 24 h incubation of **1** or **2** with **3**, and subsequent addition of **4** in the presence of Nile Red (6.25×10^{-6} M): A) bare gel, B) 1 mol% **1**, C) 3 mol% **1**, or D) 1 mol% **2**. Scale bar is 10 µm. Full videos can be found in Movies S1–S4 (Supporting Information).

of compound **4** (120×10^{-3} M) to **3** (20×10^{-3} M) with Nile Red displayed the initial formation of an emulsion with droplets of an average size of 2.87 ± 0.42 µm after 5 min (Figure 3A, 5 min), whereas no observable aggregate structures for **3** only were found by CLSM under the same conditions. Subsequently, depletion of the droplets was observed with the onset of fluorescent protrusions suggestive of fiber bundles evolving into a densely connected network, as observed previously in fully gelated samples by SEM (Figure 3A, 15–45 min, Movie S1, Supporting Information). By acquiring images every 10 s by confocal microscopy, it became clear that these droplets served as nucleation centers for the subsequent growth of the network, and the addition of a particular crosslinker affected their size and surface properties biasing the outcome of the gelation pathway of the reaction-coupled gelator. The addition of 1 mol% of **1** resulted in a decrease in the size of the individual droplets to 1.19 ± 0.26 µm, but an increase in their number after 5 min, and eventually flocculating prior to evolution of the fibrillar network based on the diffuse fluorescence emanating from the individual droplets (Figure 3B and Movie S2, Supporting

Information). When the concentration of **1** was increased to 3 mol%, the number of droplets increased to a greater extent with a decrease in size to 0.65 ± 0.15 µm after 5 min (Figure 3C, 5 min). The aggregates then clustered together becoming brighter and slightly larger in appearance, yet lacked the presumed formation of an extensive network similar to the connected spherical structures observed by SEM (Figure 3C, 15–45 min, Movie S3, Supporting Information). As a control, the addition of 1 mol% asymmetrically modified crosslinker **1** did result in small droplets similar to those observed with the fully functionalized crosslinker **1**. However, droplets functionalized with asymmetrically modified **1** did not show flocculation (Movie S5, Supporting Information), suggesting that a doubly functionalized DNA crosslinker is required to induce their bridging. In contrast, the addition of 1 mol% **2** resulted in the appearance of larger spheres with a size of 4.05 ± 0.78 µm after 5 min that became less regular and dense during the self-assembly process and eventually forming a discontinuous network in comparison to the native gel (Figure 3D and Movie S4, Supporting Information). Dynamic light scattering (DLS) measurements supported the observed changes in size by CLSM when crosslinker **1** or **2** is added to **4** (Figure S9, Supporting Information). Moreover, concentration-dependent DLS measurements of **4** supported the presence of large aggregates with emulsion-like behavior (Figure S10, Supporting Information). In all cases, the droplets were stable over the course of an hour as long as the hydrazide premonomer **3** was absent.

Most likely, the addition of the negatively charged DNA crosslinker to the droplet surface of premonomer **4** increases its charge and thereby reduces its size in parallel with increasing the concentration of the DNA crosslinker. However, the electrostatic stabilization of the droplets is short lived with the addition of **3** resulting in flocculation occurring during the formation and crosslinking of the network. In the case of 1 mol% DNA, the crosslinker exerts a positive effect on network formation through increased nucleation sites, extensive fibrillization, and formation of a robust crosslinked network due to its stiff and charged character, whereas its addition up to 3 mol% seems to prevent extensive fibrillar growth due to smaller droplet sizes. In the case of the PEG crosslinker **2**, larger stable spherical aggregates are formed with steric stabilization of the premonomer droplets of **4** by the soft and neutral polymer, but they are fewer in number relative to the native gel. This decrease in nucleation centers increases their distance, therefore decreasing the potential for the clusters of self-assembling fiber bundles to interpenetrate to form a strong network. Taken together, these results highlight that the crosslinker with its associated physicochemical properties can not only serve to reinforce the gelator network but also it can influence the early stages of the reaction-coupled gelation pathway, with both phenomena impacting the final network microstructure.

The use of polymeric crosslinkers is an attractive strategy to control the properties of supramolecular polymer networks because of its facile nature. However, this method of modulating the materials properties can prove more complex as not all crosslinkers are equivalent in how they can interact with the scaffold monomers during their self-assembly process. We have shown that the incorporation of a stiff negatively charged DNA crosslinker results in the tunable increase of mechanical properties at low crosslinker concentrations (1 mol%) by oscillatory rheology. Importantly, a twofold increase was observed for the 5′-bisaldehyde DNA crosslinker over the 5′-monoaldehyde DNA crosslinker, suggestive of its incorporation into the hydrogel material as a crosslinking moiety. Alternatively, the addition of a soft and neutral PEG-based crosslinker at the same concentration or DNA at a greater concentration than 1 mol% results in samples that show decreased mechanical stiffness relative to the native material when added at the start of the self-assembly process. We used real-time imaging by CLSM (Movies S1–S4, Supporting Information) to gain insight into the formation of the reaction-coupled low molecular weight hydrogels in the presence of a given crosslinker due to the recent interest in the early stages of the self-assembly process on various supramolecular polymers and hydrogelators.[45–48] Importantly, we found that in addition to functioning as a crosslinker of the network, adding a crosslinker also modulates the size and surface chemistry of the spherical aggregates that act as depots of unreacted building block **4**, dictating the self-assembly pathway of the low molecular weight gelator material over the various stages of nucleation, fiber growth, and bundling (**Scheme 2**).

The overarching goal to prepare modular, functional supramolecular materials for a broad range of applications requires the incorporation of tethered (bio)molecules or polymers with a wide variety of chemical and physical properties. Based on our results, careful consideration of the physicochemical features of the functional cargo becomes critical due to its potential for interaction with the early stage assemblies during the self-assembly process and its effect on the mechanical properties of the final material. Although caution must be exercised to provide an adequate balance between functionality and scaffold

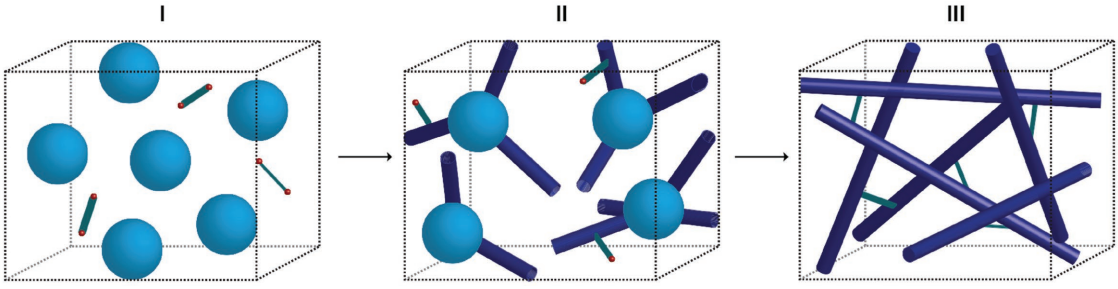

Scheme 2. Schematic representation of network formation of **1** or **2** with **3** and **4** over time, in which spherical aggregates of **4** (light blue) act as nucleation centers (I) for fibrillar growth (dark blue) incorporating the physicochemically distinct crosslinker moieties (green/red) (II) to form an interpenetrated network (III) and macroscopic hydrogel material.

integrity in these reaction-coupled noncovalent materials for their widespread application, this work reveals new opportunities for control over their properties.

Experimental Section

Experimental details including synthetic procedures and characterizations, oscillatory rheology, Avrami analysis, scanning electron microscopy, dynamic light scattering, confocal laser scanning microscopy, and cryogenic transmission electron microscopy are documented in the Supporting Information.

Supporting Information

Supporting Information is available from the Wiley Online Library or from the author.

Acknowledgements

The authors would like to thank G. Lamers (SEM), R. I. Koning and B. Koster (cryo-EM), and D. Kraft for discussion. R.E.K. would like to acknowledge the Netherlands Organisation for Scientific Research (NWO) for her VENI grant. R.E. would like to acknowledge NWO for his VIDI grant.

Received: July 16, 2016
Published online: January 24, 2017

[1] T. Aida, E. W. Meijer, S. I. Stupp, *Science* **2012**, *335*, 813.
[2] X. Du, J. Zhou, J. Shi, B. Xu, *Chem. Rev.* **2015**, *115*, 13165.
[3] E. Krieg, M. M. C. Bastings, P. Besenius, B. Rybtchinski, *Chem. Rev.* **2016**, *116*, 2414.
[4] E. Appel, J. del Barrio, X. J. Loh, O. A. Scherman, *Chem. Soc. Rev.* **2012**, *41*, 6195.
[5] C. H. Pape, M. M. C. Bastings, R. E. Kieltyka, H. M. Wyss, I. K. Voets, E. W. Meijer, P. Y. W. Dankers, *Int. J. Mol. Sci.* **2014**, *15*, 1096.
[6] D. J. Cornwell, D. K. Smith, *Mater. Horiz.* **2015**, *2*, 279.
[7] A. E. Way, A. B. Korpusik, T. B. Dorsey, L. E. Buerkle, H. A. Von Recum, S. J. Rowan, *Macromolecules* **2014**, *47*, 1810.
[8] C. Yan, D. J. Pochan, *Chem. Soc. Rev.* **2010**, *39*, 3528.
[9] E. T. Pashuck, H. Cui, S. I. Stupp, *J. Am. Chem. Soc.* **2010**, *132*, 6041.
[10] X. Zhang, X. Chu, L. Wang, H. Wang, G. Liang, J. Zhang, J. Long, Z. Yang, *Angew. Chem. Int. Ed.* **2012**, *51*, 4388.
[11] R. E. Kieltyka, A. C. H. Pape, L. Albertazzi, Y. Nakano, M. M. C. Bastings, I. K. Voets, P. Y. W. Dankers, E. W. Meijer, *J. Am. Chem. Soc.* **2013**, *135*, 11159.
[12] Y. Li, Y. Ding, M. Qin, Y. Cao, W. Wang, *Chem. Commun.* **2013**, *49*, 8653.
[13] M. M. E. Koenigs, A. Pal, H. Mortazavi, G. M. Pawar, C. Storm, R. P. Sijbesma, *Macromolecules* **2014**, *47*, 2712.
[14] M. A. Khalily, M. Goktas, M. O. Guler, *Org. Biomol. Chem.* **2015**, *13*, 1983.
[15] V. D. Nguyen, A. Pal, F. Snijkers, M. Colomb-Delsuc, G. Leonetti, S. Otto, J. van der Gucht, *Soft Matter* **2016**, *12*, 432.
[16] R. N. Shah, N. A. Shah, M. M. Del Rosario Lim, C. Hsieh, G. Nuber, S. I. Stupp, *Proc. Natl. Acad. Sci. USA* **2010**, *107*, 3293.
[17] A. Baral, S. Roy, A. Dehsorkhi, I. W. Hamley, S. Mohapatra, S. Ghosh, A. Banerjee, *Langmuir* **2014**, *30*, 929.
[18] V. Jayawarna, M. Ali, T. A. Jowitt, A. F. Miller, A. Saiani, J. E. Gough, R. V. Ulijn, *Adv. Mater.* **2006**, *18*, 611.
[19] J. P. Jung, J. Z. Gasiorowski, J. H. Collier, *Biopolymers* **2010**, *94*, 49.
[20] Z. Yang, G. Liang, L. Wang, B. Xu, *J. Am. Chem. Soc.* **2006**, *128*, 3038.
[21] J. A. Sáez, B. Escuder, J. F. Miravet, *Tetrahedron* **2010**, *66*, 2614.
[22] Z. Yang, B. Xu, *Chem. Commun.* **2004**, 2424.
[23] M. Ikeda, T. Tanida, T. Yoshii, K. Kurotani, S. Onogi, K. Urayama, I. Hamachi, *Nat. Chem.* **2014**, *6*, 511.
[24] J. D. Tovar, *Acc. Chem. Res.* **2013**, *46*, 1527.
[25] S. R. Diegelmann, J. M. Gorham, J. D. Tovar, *J. Am. Chem. Soc.* **2008**, *130*, 13840.
[26] J. Raeburn, D. J. Adams, *Chem. Commun.* **2015**, *51*, 5170.
[27] Y. Ohsedo, *Gels* **2016**, *2*, 13.
[28] J. Raeburn, A. Z. Cardoso, D. J. Adams, *Chem. Soc. Rev.* **2013**, *42*, 5143.
[29] J. H. Van Esch, *Langmuir* **2009**, *25*, 8392.
[30] J. L. Li, X. Y. Liu, *Adv. Funct. Mater.* **2010**, *20*, 3196.
[31] R. Wang, X.-Y. Liu, J. Xiong, J. Li, *J. Phys. Chem. B* **2006**, *110*, 7275.
[32] L. E. Buerkle, S. J. Rowan, *Chem. Soc. Rev.* **2012**, *41*, 6089.
[33] G. Pont, L. Chen, D. G. Spiller, D. J. Adams, *Soft Matter* **2012**, *8*, 7797.
[34] Z. Yang, B. Xu, *Adv. Mater.* **2006**, *18*, 3043.
[35] S. Toledano, R. J. Williams, V. Jayawarna, R. V. Ulijn, *J. Am. Chem. Soc.* **2006**, *128*, 1070.
[36] J. Boekhoven, J. M. Poolman, C. Maity, F. Li, L. van der Mee, C. B. Minkenberg, E. Mendes, J. H. van Esch, R. Eelkema, *Nat. Chem.* **2013**, *5*, 433.
[37] Y. H. Roh, R. C. H. Ruiz, S. Peng, J. B. Lee, D. Luo, *Chem. Soc. Rev.* **2011**, *40*, 5730.
[38] N. C. Seeman, *Nature* **2003**, *421*, 427.
[39] T. R. Wilks, J. Bath, J. W. de Vries, J. E. Raymond, A. Herrmann, A. J. Turberfield, R. K. O'Reilly, *ACS Nano* **2013**, *7*, 8561.
[40] L. Peng, C. Wu, M. You, D. Han, Y. Chen, T. Fu, M. Ye, W. Tan, *Chem. Sci.* **2013**, *4*, 1928.
[41] H. Lee, R. M. Venable, A. D. Mackerell, R. W. Pastor, *Biophys. J.* **2008**, *95*, 1590.
[42] J. K. Armstrong, R. B. Wenby, H. J. Meiselman, T. C. Fisher, *Biophys. J.* **2004**, *87*, 4259.
[43] J. M. Poolman, J. Boekhoven, A. Besselink, A. G. L. Olive, J. H. van Esch, R. Eelkema, *Nat. Protoc.* **2014**, *9*, 977.
[44] X. Y. Liu, P. D. Sawant, *Adv. Mater.* **2002**, *14*, 421.
[45] A. Z. Cardoso, L. L. E. Mears, B. N. Cattoz, P. C. Griffiths, R. Schweins, D. J. Adams, *Soft Matter* **2016**, *12*, 3612.
[46] A. Levin, T. O. Mason, L. Adler-Abramovich, A. K. Buell, G. Meisl, C. Galvagnion, Y. Bram, S. A. Stratford, C. M. Dobson, T. P. J. Knowles, E. Gazit, *Nat. Commun.* **2014**, *5*, 5219.
[47] G. Fichman, T. Guterman, J. Damron, L. Adler-Abramovich, J. Schmidt, E. Kesselman, L. J. W. Shimon, A. Ramamoorthy, Y. Talmon, E. Gazit, *Sci. Adv.* **2016**, *2*, e1500827.
[48] Y. M. Abul-Haija, S. Roy, P. W. J. M. Frederix, N. Javid, V. Jayawarna, R. V Ulijn, *Small* **2014**, *10*, 973.